

Swift observations of unidentified radio sources in the revised Third Cambridge Catalogue

A. Maselli,¹ F. Massaro,^{2,3,4} G. Cusumano,¹ V. La Parola,¹ D. E. Harris^{†, 5},
A. Paggi,⁵ E. Liuzzo,⁶ G. R. Tremblay,⁷ S. A. Baum,^{8,9} and C. P. O’Dea^{8,10}

¹INAF-IASF Palermo, via U. La Malfa 153, I-90146 Palermo, Italy

²Dipartimento di Fisica, Università degli Studi di Torino, via Pietro Giuria 1, I-10125 Torino, Italy

³Istituto Nazionale di Fisica Nucleare, Sezione di Torino, via Pietro Giuria 1, I-10125 Torino, Italy

⁴INAF-Osservatorio Astronomico di Roma, Via di Frascati 33, I-00040 Monte Porzio Catone, RM, Italy

⁵Harvard-Smithsonian Astrophysical Observatory, 60 Garden Street, Cambridge, MA 02138, USA

⁶INAF-Istituto di Radioastronomia, via Gobetti 101, 40129, Bologna, Italy

⁷Yale Center for Astronomy and Astrophysics, Physics Department, Yale University, P.O. Box 208120, New Haven, CT 06520-8120, USA

⁸University of Manitoba, Dept. of Physics and Astronomy, Winnipeg, MB R3T 2N2, Canada

⁹Carlson Center for Imaging Science 76-3144, 84 Lomb Memorial Drive, Rochester, NY 14623, USA

¹⁰School of Physics and Astronomy, Rochester Institute of Technology, 84 Lomb Memorial Drive, Rochester, NY 14623, USA

Accepted 2016 May 18. Received 2016 May 18; in original form 2016 March 18

ABSTRACT

We have investigated a group of unassociated radio sources included in the 3CR catalogue to increase the multi-frequency information on them and possibly obtain an identification. We have carried out an observational campaign with the *Swift* satellite to observe with the UVOT and the XRT telescopes the field of view of 21 bright NVSS sources within the positional uncertainty region of the 3CR sources. Furthermore, we have searched in the recent AllWISE Source Catalogue for infrared sources matching the position of these NVSS sources. We have detected significant emission in the soft X-ray band for nine of the investigated NVSS sources. To all of them, and in four cases with no soft X-ray association, we have associated a *WISE* infrared counterpart. Eight of these infrared candidates have not been proposed earlier in the literature. In the five remaining cases our candidate matches one among a few optical candidates suggested for the same 3CR source in previous studies. No source has been detected in the UVOT filters at the position of the NVSS objects, confirming the scenario that all of them are heavily obscured. With this in mind, a spectroscopic campaign, preferably in the infrared band, will be necessary to establish the nature of the sources that we have finally identified.

Key words: galaxies: active – radio continuum: galaxies – radiation mechanisms: non-thermal – X-rays: general

1 INTRODUCTION

The extragalactic subset of the revised Third Cambridge Catalogue (3CR) of radio sources (see, *e.g.*, ??) has a long history as one of the fundamental samples used to understand the nature and evolution of powerful radio galaxies and quasars, as well as their relationship to their host galaxies and environments on parsec through megaparsec scales. Extensive imaging and spectroscopic observations have long

been available from the radio through the infrared (IR) and optical bands, with data from *Spitzer* (?), the *Hubble Space Telescope* (*e.g.*, ??) and ground-based telescopes (see, *e.g.*, the description of observations performed with the Telescopio Nazionale Galileo reported in ?).

Since a large fraction of 3CR sources were already present in both the *Chandra* (see, *e.g.*, ?, for a recent review) and *XMM-Newton* archives of pointed observations (*e.g.* ?, and references therein), in 2008 a *Chandra* snapshot survey started to complete the X-ray coverage of the entire 3CR extragalactic catalogue (???). This *Chandra* survey has enabled investigations of peculiar sources (see, *e.g.*, ? for 3C 17 and ? for 3C 105), samples of radio-loud objects (?), and was the genesis of, *e.g.*, follow-up X-ray observations for

† Dan Harris passed away on December 6th, 2015. His career spanned much of the history of radio and X-ray astronomy. His passion, insight, and contributions will always be remembered.

Table 1. The list of unidentified 3CR sources, with the corresponding NVSS source, when present. 1) The 3C designation; 2-3) Right Ascension (J2000) with its rms uncertainty; 4-5) Declination (J2000) with its rms uncertainty; 6-7) Galactic Longitude and Latitude (J2000); 8) flux density at 178 MHz, corrected following Laing et al. (1983); 9-10) corresponding NVSS source, with its flux density at 1.4 GHz; 11) radio spectral index α computed in the range 178 MHz-1.4 GHz.

3C	R.A. (hh mm ss)	Error (s)	Dec. (dd mm ss)	Error (arcmin)	l (deg)	b (deg)	S_{178} (Jy)	NVSS	$S_{1.4}$ (Jy)	α
11.1	00 29 56.43	18.0	+63 40 34.2	45.0	120.55	+0.90	13.5	J002945+635841	2.99	0.73
14.1	00 36 27.13	18.0	+59 46 30.3	45.0	121.04	-3.04	17.5	-	-	-
21.1	00 45 35.25	18.0	+68 04 23.5	45.0	122.38	+5.21	9.8	-	-	-
33.2	01 10 19.72	18.0	+69 21 57.4	60.0	124.61	+6.56	6.0	-	-	-
86	03 27 20.10	2.0	+55 18 49.7	1.0	143.91	-1.08	31.6	J032719+552029	6.94	0.73
91	03 37 42.67	2.5	+50 45 45.1	3.0	147.81	-3.90	15.4	J033743+504552	3.34	0.74
125	04 46 16.16	5.0	+39 42 23.9	7.0	164.14	-3.69	15.4	J044617+394503	2.02	0.98
131	04 53 22.56	3.0	+31 27 47.9	3.0	171.46	-7.82	15.9	J045323+312924	2.87	0.83
134	05 04 42.19	1.0	+38 06 12.7	1.0	167.64	-1.90	81.1	J050443+380539	2.14	1.05
137	05 19 32.65	3.0	+50 55 40.3	3.0	158.78	+7.76	13.6	J051932+505432	2.07	0.91
139.2	05 24 28.20	3.0	+28 13 41.5	3.0	178.06	-4.29	13.0	J052427+281255	0.29	0.94
141	05 26 42.60	1.5	+32 49 32.1	2.5	174.54	-1.32	16.2	J052642+324958	2.17	0.97
152	06 04 29.42	3.0	+20 21 10.9	3.0	189.57	-0.64	13.5	J060428+202122	1.86	0.96
158	06 21 40.95	5.0	+14 29 31.5	8.0	196.68	+0.15	19.7	J062141+143211	2.24	1.05
250	11 08 52.12	3.0	+25 00 54.2	3.0	212.37	+66.91	9.6	J110851+250052	1.09	1.05
389	18 46 18.63	7.0	-03 19 44.5	12.0	29.38	-0.38	22.9	-	-	-
390	18 45 34.41	3.0	+09 52 12.9	4.0	41.08	+5.77	22.9	J184537+095344	4.51	0.79
394	18 59 20.89	6.0	+13 00 11.8	7.0	45.42	+4.17	16.5	J185923+125912	2.88	0.85
399.1	19 15 56.83	3.0	+30 20 02.1	3.0	62.73	+8.53	14.7	J191556+301952	2.97	0.78
409	20 14 27.74	1.0	+23 34 58.4	2.0	63.40	-6.12	83.5	J201427+233452	13.68	0.88
415.2	20 32 50.51	3.0	+53 45 46.1	3.0	90.27	+8.19	9.6	J203246+534553	1.01	1.09
428	21 08 25.59	3.0	+49 34 05.7	3.0	90.50	+1.28	18.1	J210822+493637	2.41	0.98
431	21 18 55.56	3.0	+49 34 18.2	3.0	91.68	+0.05	26.4	J211852+493658	3.39	1.00
454.2	22 52 15.62	18.0	+65 03 57.3	45.0	110.79	+5.04	9.6	J225205+644010	2.29	0.69
468.1	23 50 54.76	18.0	+64 40 19.0	45.0	116.51	+2.56	32.7	J235054+644018	4.95	0.92

3C 89 (Dasadia et al. 2015), 3C 171 (?), and 3C 305 (??). The total number of 3CR extragalactic sources now present in the Chandra archive is 248 out of the 298 included in the update of the 3CR catalogue performed by ?. An additional 16 sources (out of 50) that remain unobserved by *Chandra* have recently been approved for observation in Cycle 17 (see Massaro et al. 2016). Those observations began as of December 2015.

Amid our investigation of recent *Chandra* observations, we realised that 25 out of the 298 3CR radio sources are not only unobserved in X rays, but are in fact completely *unidentified*, lacking an assigned optical or infrared counterpart. In the latest revised release of 3CR extragalactic catalogue (?), each of these 25 unidentified sources (excluding 3C 86 and 3C 415.2) are marked as *obscured* active galaxies. This classification has remained unchanged for the past three decades, save for a few tentative associations requiring follow-up observations for confirmation (see, *e.g.*, ??). It therefore became necessary, in nearing completion of the 3CR *Chandra* snapshot survey, to enact an ancillary optical-to-X-ray campaign with the *Swift* observatory in order to better characterise the properties of these unidentified sources. Our *Swift* campaign was augmented by a search for infrared counterparts in the latest AllWISE Source Catalogue from the Wide-field Infrared Survey Explorer (WISE, ?) mission.

Here we present the results of this new observational effort. Our *Swift* observing strategy is described in § 2, the reduction and analysis of *Swift* X-ray data is discussed in § 3, and the search for infrared and optical counterparts is

described in § 4. Our results, including detections of both infrared and soft X-ray counterparts, are given in § 5 and summarised in § 6. Throughout this paper we use CGS units, unless stated otherwise. The spectral index α is defined in terms of the flux density S_ν , where $S_\nu \propto \nu^{-\alpha}$ and ν is the frequency.

2 OBSERVING STRATEGY

The coordinates of the 3CR sources were first provided by ? and later modified up to the most recent update carried out by ?. In several cases, including a few sources of interest, the positional uncertainty reaches values up to 60 arcmin in Declination. Given the high flux density threshold used in selecting sources for the 3CR catalogue, we have assumed that a bright source in the more recent NRAO VLA Sky Survey (NVSS, ?) at 1.4 GHz would be associated with all unidentified 3CR sources. The positional uncertainty of NVSS objects with flux density values higher than 100 mJy is always lower than one arcsecond. The 3CR catalogue included sources with flux density values S_{178} higher than 9 Jy: considering the radio spectral index distribution of unidentified 3CR sources reported by ?, we have established a lower limit of $S_{1.4}^* = 1$ Jy for the expected flux density at 1.4 GHz. Therefore, to establish the most suited coordinates to be used in our *Swift* campaign, we have searched for NVSS sources with $S_{1.4} > S_{1.4}^*$.

In most cases the result of our search was a single NVSS source with a compact radio morphology. In two cases (for 3C 134 and 3C 139.2) we found a group of three catalogued objects that in actuality correspond to the same radio source

Table 2. The list of *Swift*-XRT detected sources matching one of the NVSS sources listed in Table 1. 1) The 3C designation; 2-3) Equatorial coordinates of the X-ray source; 4) error radius; 5) XRT exposure time; 6) XRT count rate with its error; 7) significance of the X-ray detection; 8) corresponding NVSS source; 9) angular separation between the X-ray and the radio source.

3C	R.A.(J2000)	Dec. (J2000)	Error (arcsec)	Exposure (s)	Count Rate (ct/s)	S/N (σ)	NVSS	Angular Separation (arcsec)
86	03 27 19.5	+55 20 26.0	4.5	5170	$(1.43 \pm 0.19) \cdot 10^{-2}$	7.6	J032719+552029	3.7
91	03 37 43.0	+50 45 46.2	4.0	4809	$(4.39 \pm 0.39) \cdot 10^{-2}$	11.3	J033743+504552	7.4
131	04 53 23.2	+31 29 33.4	6.3	5255	$(1.96 \pm 0.74) \cdot 10^{-3}$	2.6	J045323+312924	9.4
137	05 19 32.6	+50 54 31.4	4.7	5092	$(9.98 \pm 1.60) \cdot 10^{-3}$	6.1	J051932+505432	1.9
158	06 21 41.2	+14 32 11.5	6.4	4974	$(2.04 \pm 0.78) \cdot 10^{-3}$	2.6	J062141+143211	1.6
390	18 45 37.6	+09 53 48.7	4.4	4348	$(2.60 \pm 0.30) \cdot 10^{-2}$	8.6	J184537+095344	4.4
409	20 14 27.5	+23 34 54.5	4.0	5366	$(3.27 \pm 0.28) \cdot 10^{-2}$	11.6	J201427+233452	1.9
428	21 08 22.1	+49 36 42.1	4.6	7913	$(7.79 \pm 1.10) \cdot 10^{-3}$	6.9	J210822+493637	5.6
454.2	22 52 05.2	+64 40 13.1	4.6	5571	$(7.76 \pm 1.40) \cdot 10^{-3}$	5.6	J225205+644010	4.6

- both of these are radio galaxies with Fanaroff-Riley class II (FR II, ?) morphology (?), that NVSS has spatially resolved into a radio core and two jet hotspots. For both of these FR II sources (see, *e.g.*, Fig.11) only one of the NVSS sources is internal to the 3CR positional uncertainty region. We note that for 3C 139.2 the flux density of the NVSS object (presumably the radio core) within the 3CR positional uncertainty region is lower than $S_{1.4}^*$, but we have nevertheless included it in our observational campaign considering the contribution of the two hotspots (0.7 Jy and 0.9 Jy, respectively) to the total flux. We have also decided to include three NVSS objects with an angular separation of a few arcseconds from the closest side of the corresponding 3CR positional uncertainty region: 1.8 and 3.4 arcsec for 3C 390 and 3C 428, respectively, and ~ 39 arcsec for 3C 86. In these cases, as a consequence of this small angular separation, the NVSS radio contours (up to 10 mJy beam $^{-1}$) largely overlap the corresponding 3CR positional uncertainty region. On the other hand, we have excluded 3C 14.1, 3C 21.1, 3C 33.2, and 3C 389 from our initial dataset as we have found no bright NVSS source in or near (within several arcminutes) the corresponding 3CR positional uncertainty region.

The list of these 21 previously unassociated 3CR sources is given in Table 1. For each, we report the Equatorial coordinates with their statistical uncertainty, the Galactic coordinates, their flux density at 178 MHz, the corresponding NVSS source with its flux density at 1.4 GHz, and the radio spectral index α computed between 178 MHz and 1.4 GHz. The flux density values at 178 MHz include a 9 per cent correction factor (?) to those originally provided by ? and also reported by ?. For both 3C 134 and 3C 139.2 only the NVSS object internal to the 3CR positional uncertainty region has been reported in Table 1; however, in the computation of the radio spectral index α we have included the contribution of the additional NVSS objects that correspond to the same radio galaxy, under the assumption that the older survey at 178 MHz was unable to spatially resolve them.

3 X-RAY DATA REDUCTION AND ANALYSIS PROCEDURES

Each of these 21 NVSS sources was covered by our *Swift* observational campaign, carried out between November 2014 and March 2015, with a total exposure time greater than 4 ks for each source. The X-ray data reduction and procedures adopted in the present analysis were extensively described in ???, and references therein; here we report only the basic details (see also ?? for further details).

The XRT data have been processed with the XRTDAS software package (v.3.0.0) developed at the ASI Science Data Center (ASDC) and distributed within the HEASoft package (v.6.16) by the NASA High Energy Astrophysics Archive Research Center (HEASARC). All the XRT observations were carried out in the most sensitive photon counting (PC) read-out mode. Event files have been calibrated and cleaned applying standard filtering criteria with the XRTPIPELINE task and using the latest calibration files available in the Swift CALDB distributed by HEASARC. Events in the energy range 0.3–10 keV with grades 0–12 have been used in the analysis. Exposure maps have been also created with XRTPIPELINE. The detection of X-ray sources in the XRT images has been carried out using the detection algorithm DETECT within XIMAGE. In agreement with ?, we have set the DETECT signal-to-noise ratio acceptance threshold to 2.5σ . Finally, the positional uncertainty (90 per cent confidence level) of each detected source has been computed using the XRTCENTROID task. When needed, we have computed a 3σ upper limit of the count rate at the desired coordinates using the UPLIMIT command within XIMAGE. Source count rate photometry was conducted using square boxes with half-size of 7 pixels, while background intensity was set to a constant equal to the average value computed over the whole image.

The list of XRT sources that we have detected following the above described procedure and matching one NVSS source is reported in Table 2, for a total of nine X-ray sources. For each, we report the corresponding 3CR source (column 1), its Right Ascension (column 2) and Declination (column 3), the error radius (column 4), the XRT exposure time (column 5), the count rate with its error (column 6), the significance of its detection (column 7), the corresponding NVSS source (column 8) and the angular separation from its

Table 3. The list of the NVSS sources with no matching X-ray detection and the corresponding *Swift* -XRT 3σ upper limit.

3C	NVSS	Exposure (s)	3σ upper limit (ct/s)
11.1	J002945+635841	5263	$1.69 \cdot 10^{-3}$
125	J044617+394503	4132	$4.41 \cdot 10^{-3}$
134	J050443+380539	4944	$3.46 \cdot 10^{-3}$
139.2	J052427+281255	4817	$3.21 \cdot 10^{-3}$
141	J052642+324958	4651	$2.24 \cdot 10^{-3}$
152	J060428+202122	4894	$1.87 \cdot 10^{-3}$
250	J110851+250052	4280	$4.80 \cdot 10^{-3}$
394	J185923+125912	4032	$5.32 \cdot 10^{-3}$
399.1	J191556+301952	12339	$2.20 \cdot 10^{-3}$
415.2	J203246+534553	5358	$3.59 \cdot 10^{-3}$
431	J211852+493658	7462	$2.77 \cdot 10^{-3}$
468.1	J235054+644018	4997	$3.10 \cdot 10^{-3}$

position (column 9). The name adopted for these sources in this paper starts with the prefix XRT and then encodes the J2000 sky position following the standard IAU convention (*e.g.*, XRT JHHMMSS.S+DDMMSS). In three cases (3C 91, 3C 131 and 3C 428) the NVSS source has been found at an angular separation higher than the corresponding XRT error radius (see the exact values reported in Table 2). In principle, a marginal disagreement between the positions of the catalogued radio source, which is really the radio centroid weighted in position by any intrinsic asymmetry in the radio structure, and of the detected X-ray source (which should mark the AGN position more precisely) is not unexpected. Considering this, and the fact that the XRT error radius is given at a 90 per cent confidence level, in the first instance we have not rejected the match and we have later verified the possible agreement of the X-ray object with the position of a *WISE* object (see Section 4) rather than the NVSS one. Further detected X-ray sources were found at much higher angular separations from the catalogued NVSS objects, so that any relation between them could be safely excluded. Regarding the twelve NVSS sources for which no significant (higher than 2.5σ) X-ray detection has been found, a 3σ upper limit has been computed at the position corresponding to the NVSS coordinates; the list of these is reported in Table 3.

4 SEARCH FOR INFRARED AND OPTICAL COUNTERPARTS

We have searched for infrared counterparts to the NVSS sources reported in Table 1 by cross-matching this list with the AllWISE Source Catalogue. Following ?, we have used the value of 3.3 arcsec as proper matching radius. In the previously cited cases of 3C 91, 3C 131 and 3C 428 (see Section 3), an infrared object has been found at an angular separation higher than 3.3 arcsec from the NVSS object (exact values are shown in Table 4, described below), which is nevertheless still within the error circle of the corresponding XRT source. Having found positional agreement between the infrared and the soft X-ray objects, with only a modest difference with respect to the NVSS coordinates, we accept these objects as counterparts of the same source.

As a result of our analysis, an infrared counterpart has been found for all sources reported in Table 2, as well as in four additional cases among the X-ray non-detections listed in Table 3. Their list is reported in Table 4, according to the presence/absence of an X-ray counterpart. For each infrared source we have reported the corresponding 3CR (column 1) and NVSS (column 2) sources, the name in the AllWISE Catalogue (column 3), the angular separation from the radio (column 4) and the X-ray source (column 5), and the corresponding magnitudes in the *WISE* filters (columns 6–9).

We have also carried out a photometric analysis over the images in the available UVOT filters at the position of the NVSS sources. Following ?, the photometry has been performed using the UVOTDETECT task and taking into account the corresponding exposure maps. An extraction region of 5 arcsec has been adopted for the sources, independently of the image filter, and a larger circle of 20 arcsec radius for the background, in a near source-free region of the sky. Magnitude values, or upper limits, in the Vega System have been finally obtained using the UVOTSOURCE task and adopting a 3σ level of significance to compute the background limit; both statistic and systematic errors have been taken into account. Our photometric results show that an optical-UV counterpart has not been detected for any object; only upper limits could be established. This result was not unexpected, considering that almost all of these sources were marked as *obscured* by ?, and nearly all are at low Galactic latitude ($|b| < 10^\circ$, see Table 1).

5 SOURCE DETAILS

In this Section we describe details of the 13 radio sources listed in Table 4, distinguishing the presence (Section 5.1) or the absence (Section 5.2) of an X-ray counterpart in addition to the infrared one. For each radio source we show a comparison of the field of view in both the XRT 0.3–10 keV band and in *WISE* *w1* filter (figures 1 to 13). The images have been smoothed with a Gaussian function with different values of FWHM (5 and 1 arcsec for the XRT and *WISE* images, respectively). In each panel a yellow dashed line marks the positional uncertainty region of the 3CR source. White crosses mark the position of the catalogued NVSS objects, and white continuous lines are used to shape the radio contours that have been obtained from the NVSS maps. The exact values of the contour levels, starting from 10 mJy beam⁻¹, have been reported for each in the corresponding captions. The positions of the X-ray sources and the corresponding error radius (see column 3 of Table 2) have been marked with red circles. The range of the image in the XRT band (left panel) has been generally chosen to cover the whole 3CR positional uncertainty region and the corresponding NVSS source with its contours; in two cases (3C 454.2 and 3C 468.1) this was not convenient due to the large extent in Declination of the positional uncertainty region. The image in the *WISE* *w1* filter shows a smaller field of view in order to aid viewing of the possible infrared counterpart.

Table 4. The *WISE* counterparts associated to some of the NVSS sources reported in Table 2.

3C	NVSS	<i>WISE</i>	WISE/NVSS (arcsec)	WISE/XRT (arcsec)	w_1 (mag)	w_2 (mag)	w_3 (mag)	w_4 (mag)
86	J032719+552029	J032719.29+552028.2	0.9	2.7	13.421±0.027	12.500±0.026	9.757±0.050	7.274±0.128
91	J033743+504552	J033743.02+504547.6	6.1	1.4	11.885±0.022	10.802±0.021	7.936±0.020	5.507±0.038
131	J045323+312924	J045323.34+312928.4	4.0	5.4	14.981±0.041	14.779±0.082	12.306	8.300
137	J051932+505432	J051932.53+505431.3	1.5	0.7	13.967±0.027	12.896±0.028	9.968±0.053	7.194±0.116
158	J062141+143211	J062141.01+143212.8	1.5	3.6	15.133±0.046	13.953±0.043	11.131±0.189	8.639±0.417
390	J184537+095344	J184537.60+095345.0	0.9	3.8	12.546±0.043	11.575±0.024	9.150±0.029	6.874±0.088
409	J201427+233452	J201427.59+233452.6	0.3	2.1	13.547±0.050	12.377±0.027	9.005±0.027	6.437±0.065
428	J210822+493637	J210822.08+493641.6	5.3	0.5	14.559±0.064	13.097±0.035	10.143±0.056	7.601±0.136
454.2	J225205+644010	J225205.50+644011.9	2.3	4.6	14.652±0.030	14.341±0.042	13.121±0.467	9.513
125	J044617+394503	J044617.88+394504.5	1.6	—	15.645±0.052	15.228±0.092	10.605±0.100	7.825±0.189
139.2	J052427+281255	J052427.51+281256.7	1.5	—	15.782±0.060	14.954±0.086	9.475±0.046	5.987±0.051
152	J060428+202122	J060428.62+202121.7	0.8	—	16.334±0.096	16.576±0.337	12.245±0.450	8.229
468.1	J235054+644018	J235054.78+644018.1	1.3	—	15.135±0.040	13.452±0.029	9.946±0.044	7.966±0.138

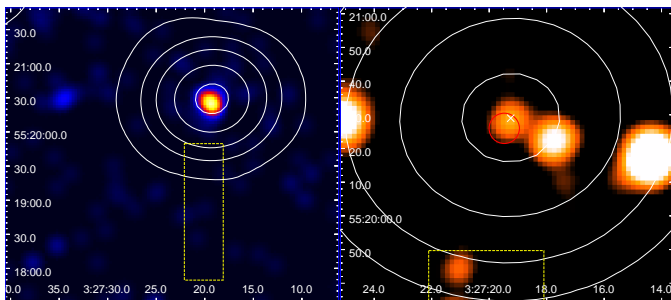


Figure 1. The sky map in the direction of **3C 86** obtained by XRT in the 0.3–10 keV energy band (left panel) and by *WISE* in the w_1 filter (right panel). A yellow dashed line marks the positional uncertainty region of the 3CR source. White continuous lines shape the radio contours obtained from the NVSS map and corresponding to 0.01, 0.2, 0.7, 2, and 4 Jy beam⁻¹; a white cross marks the position of the catalogued NVSS source. A red circle marks the position of the detected XRT source with the corresponding error radius.

5.1 3CR sources with both X-ray and infrared counterparts

5.1.1 3C 86

As shown in the left panel of Fig. 1 the 1.4 GHz source corresponding to 3C 86, NVSS J032719+552029 ($S_{1.4}=6.9$ Jy), is out of the 3CR positional uncertainty region but its radio contours overlap it. We have detected X-ray emission (XRT J032719.5+552026) cospatial with the radio source at $S/N=7.6$ and with a mean count rate of the order of 10^{-2} ct/s. Furthermore, at an angular separation of 0.9 arcsec from the NVSS coordinates, an infrared counterpart *WISE* J032719.29+552028.2 has been found in the All-*WISE* Source Catalogue with clear detections in all four *WISE* filters. This is the same counterpart reported by ? in their investigation of three 3CR sources including a spectroscopic analysis: unfortunately, the spectrum they obtained had very low signal-to-noise ratio, showing only faint continuum.

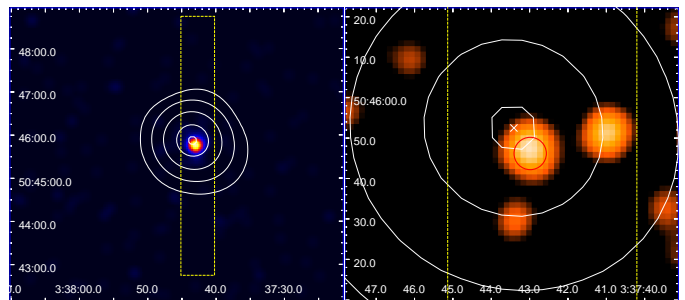


Figure 2. Same as Fig. 1 but for **3C 91**. White contours correspond in this case to 0.01, 0.1, 0.5, 1.5, and 2.3 Jy beam⁻¹.

5.1.2 3C 91

The X-ray source that we have detected (XRT J033743.0+504546) with $S/N=11.3$ and a mean count rate on the order of $4 \cdot 10^{-2}$ ct/s is 7.4 arcsec from the coordinates of NVSS J033743+504552 and 3.3 arcsec from the center of the 3CR positional uncertainty region, as shown in the left panel of Fig. 2. A *WISE* source, J033743.02+504547.6, has been found within the XRT error circle, at close angular separation (1.4 arcsec) from its center, and is clearly detected in all *WISE* filters. Considering the good positional agreement between the infrared and the X-ray objects and their low angular separation from the NVSS object (see the right panel of Fig. 2), we have accepted these as counterparts of the same source at different frequencies. Three candidates were noted by ? in their analysis of the optical images obtained by the Wide Field Planetary Camera 2 (WFPC2) on board the *Hubble Space Telescope* (HST). The angular separation between their candidate #1 (R.A. $03^h 37^m 42.93^s$; Dec. $+50^\circ 45' 48.13''$), which they considered as the most probable, and *WISE* J033743.02+504547.6 is 1.0 arcsec. ? reported for their candidate #1 an observed magnitude of $R_{obs}=19.36$ mag; there is no detection in the available UVOT filters (M_2 , W_1 , and W_2) at the corresponding position. Finally, we report that *WISE* J033743.02+504547.6

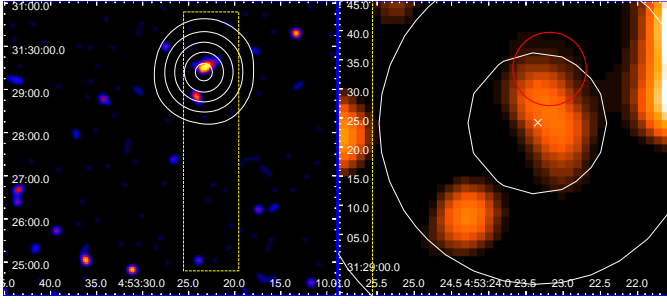


Figure 3. Same as Fig. 1 but for **3C 131**. White contours correspond in this case to 0.01, 0.1, 0.4, 1, and 1.8 Jy beam⁻¹.

has been included by ? in their all-sky catalogue of infrared selected, radio-loud active galaxies due to its peculiar infrared colours.

5.1.3 3C 131

The X-ray source XRT J045323.2+312933 has been detected at 9.4 arcsec from the coordinates of NVSS J045323+312924. There are two *WISE* objects at close angular separation (~ 4 arcsec) from the NVSS source: in the image shown in Fig. 3 (right panel) they are not resolved, and reliable magnitude values of both targets are only available for the $w1$ and $w2$ filters in the AllWISE Source Catalogue. Only one, *WISE* J045323.34+312928.4, is within the error circle of the XRT source. No optical candidate counterpart was supported by ? and the only cited source was considered to be unrelated to the radio structure. This region of the sky was also analysed by ?, who reported a list of four objects detected by HST. The angular separation of their candidate #4 (R.A. $04^h 53^m 23.34^s$; Dec. $+31^\circ 29' 27.10''$) from *WISE* J045323.34+312928.4 is 1.3 arcsec. Due to their large angular separation from the radio coordinates they took into account, different from the NVSS ones, all the four candidates were considered by ? to be unlikely the optical counterpart of the radio source. However, the angular separation of candidate #4 from NVSS J045323+312924 is 2.9 arcsec, lower than the positional uncertainty for the HST coordinates (3 arcsec) quoted by ?. Therefore, despite a difference of a few arcseconds (exact values are reported in Table 2 and Table 4) between the positions of objects detected at different frequencies, we suggest that the most plausible counterpart to the radio source 3C 131 corresponds to *WISE* J045323.34+312928.4.

5.1.4 3C 137

The X-ray source XRT J051932.6+505431 matches the coordinates of the NVSS source J051932+505432 with an angular separation of 1.9 arcsec. Also a reliable infrared counterpart, *WISE* J051932.53+505431.3, is found at 1.5 arcsec from the NVSS coordinates and is well detected in all the *WISE* filters. The angular separation of this infrared source from the "very faint red object", quoted by ? in their search of an optical identification and hardly distinguished in their finding chart, is 3.4 arcsec.

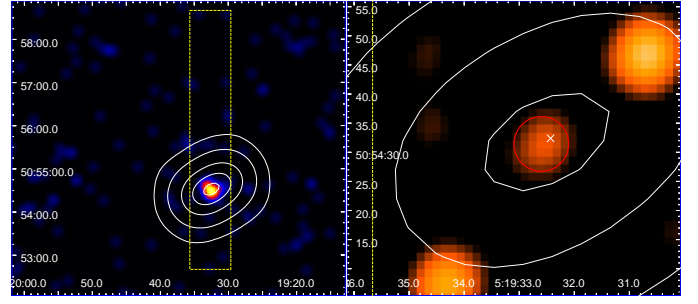


Figure 4. Same as Fig. 1 but for **3C 137**. White contours correspond in this case to 0.01, 0.1, 0.4, 0.8, and 1 Jy beam⁻¹.

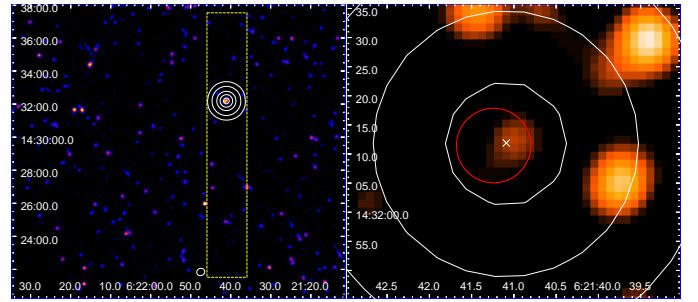


Figure 5. Same as Fig. 1 but for **3C 158**. White contours correspond in this case to 0.01, 0.1, 0.5, 1, and 1.5 Jy beam⁻¹.

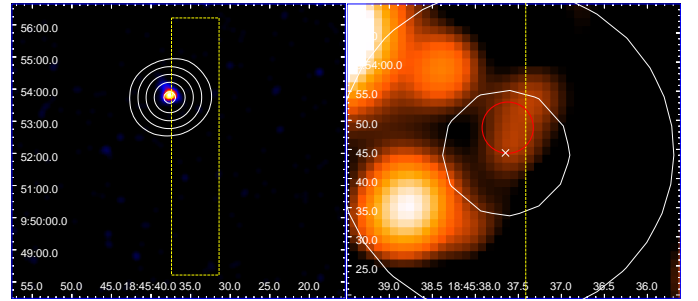


Figure 6. Same as Fig. 1 but for **3C 390**. White contours correspond in this case to 0.01, 0.1, 0.5, 1.5, and 3 Jy beam⁻¹.

5.1.5 3C 158

The X-ray source XRT J062141.2+143212 matches the NVSS source J062141+143211, within the positional uncertainty region of 3C 158, with an angular separation of 1.6 arcsec consistent with the XRT error circle. An infrared counterpart in the AllWISE Source Catalogue, *WISE* J062141.01+143212.8, is well detected in all the remaining *WISE* filters and is found at 1.5 arcsec from the NVSS source. This object, with a nice positional agreement with other sources emitting at different frequencies, is here presented for the first time as candidate to be investigated with a spectroscopic analysis; no infrared/optical candidate has been previously reported in the literature for this radio source.

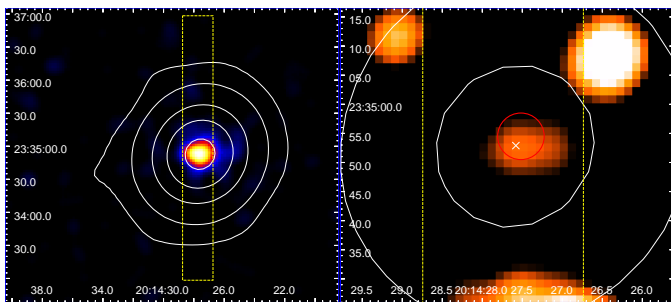


Figure 7. Same as Fig. 1 but for 3C 409. White contours correspond in this case to 0.01, 0.2, 1.5, 4, and 8 Jy beam⁻¹.

5.1.6 3C 390

The X-ray source XRT J184537.6+095349 ($S/N=8.6$) matches the radio source NVSS J184537+095344 in the field of view of 3C 390 at an angular separation of 4.4 arcsec equal to the XRT error radius. As shown in the left panel of Fig. 6 the NVSS source is not well centered with respect to the 3CR positional uncertainty region. The cross-match with the AllWISE Catalogue has provided as infrared counterpart the source *WISE* J184537.60+095345.0, at 0.9 arcsec from the NVSS coordinates. We note that there is another *WISE* source close to the one just reported; both are not fully resolved in the image shown in the right panel of Fig. 6. However, the angular separation of the latter from the NVSS source is higher (6.7 arcsec) and also larger than the established matching radius (3.3 arcsec). Moreover, we emphasise that *WISE* J184537.60+095345.0 has been recently included in the all-sky catalogue of blazar candidates by ? due to its peculiar infrared colours. Also in this case, no candidate to the radio source 3C 390 has been previously presented in the literature: a spectroscopic analysis of *WISE* J184537.60+095345.0 will finally clarify the nature of this multi-frequency source.

5.1.7 3C 409

The soft X-ray source XRT J201427.5+233455 has been detected with $S/N=11.6$ in the field of view of 3C 409 and matches the coordinates of NVSS J201427+233452 with an angular separation of 1.9 arcsec. X-ray emission in this region of the sky was indeed detected by the Imaging Proportional Counter (IPC) on board the *Einstein* satellite and reported by ?. These authors also reported of a 7.3 ks exposure with the High Resolution Imager (HRI) in which the X-ray source was located at R.A.(B1950) 20^h 12^m 18^s.42, Dec.(B1950) +23° 25′ 45″ with an uncertainty of 5 arcsec. Considering the angular separation (5.8 arcsec) of this source from XRT J201427.5+233455 the X-ray emission detected from *Einstein* and *Swift* is probably related to the same object. The match with the AllWISE Source Catalogue has provided the infrared counterpart *WISE* J201427.59+233452.6 to the NVSS source, at only 0.3 arcsec from its coordinates; this infrared object is well detected in all of the four *WISE* filters. As in other three cases found in our analysis, this *WISE* infrared object has been included in the all-sky catalogue of blazar-like radio-loud sources recently produced by ?. Apart from this,

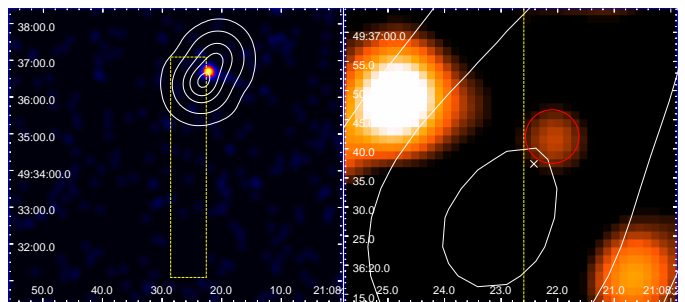


Figure 8. Same as Fig. 1 but for 3C 428. White contours correspond in this case to 0.01, 0.1, 0.4, 0.7, and 1 Jy beam⁻¹.

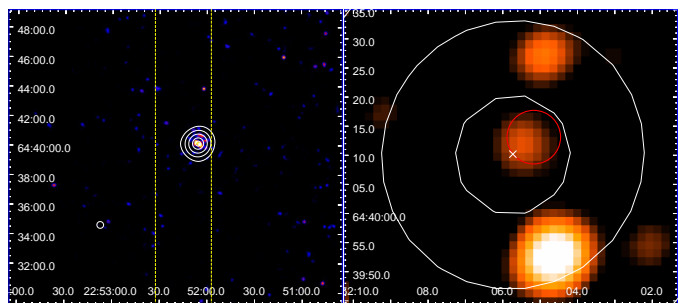


Figure 9. Same as Fig. 1 but for 3C 454.2. White contours correspond in this case to 0.01, 0.1, 0.4, 1, and 1.5 Jy beam⁻¹.

it is the first candidate ever indicated in the literature as a possible counterpart to 3C 409.

5.1.8 3C 428

The X-ray source XRT JJ210822.1+493642 matches the NVSS source J210822+493637 in the field of view of 3C 428, at an angular separation of 5.6 arcsec; the radio contours appear to be stretched in one direction (see Fig 8). As for 3C 86 and 3C 390 (see Fig.1 and Fig.6) the coordinates of the NVSS source are not well centered with respect to the 3CR positional uncertainty region: nonetheless, a substantial overlap with its radio contours is evident. From an infrared point of view a reliable infrared counterpart, *WISE* J210822.08+493641.6, has been found within the XRT error circle: the angular separation from its center is only 0.5 arcsec, much lower than the XRT error radius. The image in the *WISE* *w1* filter showing this infrared source is given in the right panel of Fig. 8; the source is well detected in all the remaining *WISE* filters. As for 3C 91, 3C 390, and 3C 409, this infrared source has been recently included in the all-sky catalogue of blazar candidates (?). Given the good match between the infrared and the X-ray source and their low angular separation with respect to the NVSS coordinates, we have finally accepted the match among these different sources indicating *WISE* J210822.08+493641.6 as the best target to be investigated with a spectroscopic campaign. We note that this position is at ~ 2 arcsec from one of the four candidates (candidate B) suggested by ? in their analysis of a CCD image obtained at the Canada-France-Hawaii Telescope (CFHT); these authors claimed for this object a magnitude $R=21.8$ mag.

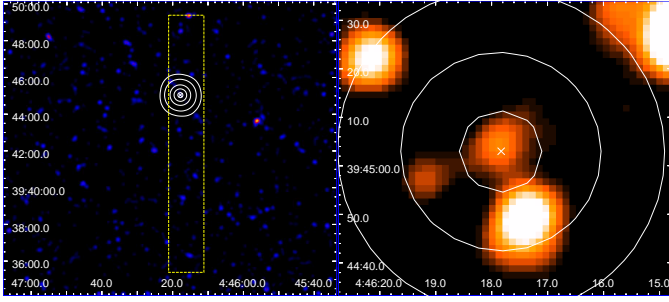


Figure 10. The sky map in the direction of **3C 125** obtained by XRT in the 0.3–10 keV energy band (left panel) and by *WISE* in the *w1* filter (right panel). A yellow dashed line marks the 3CR positional uncertainty region. White continuous lines shape the radio contours obtained from the NVSS maps and corresponding to 0.01, 0.1, 0.5, 1, and 1.4 Jy beam⁻¹; a white cross marks the position of the catalogued NVSS source.

5.1.9 3C 454.2

We have detected the soft X-ray source XRT J225205.2+644013 at 4.6 arcsec from the coordinates of the NVSS source J225205+644010 within the positional uncertainty region of 3C 454.2, as shown in the left panel of Fig. 9. At an angular separation of 2.3 arcsec from this NVSS source, consistent with the matching radius that we have established, the infrared source *WISE* J225205.50+644011.9 has been found in the AllWISE Catalogue. Excluding *w4*, it is well detected in all the remaining *WISE* filters, as reported in Table 4; the field of view in *w1* is shown in the right panel of Fig. 9. No information about infrared or optical candidates was given before in the literature about this radio source.

5.2 3CR sources with only infrared counterparts

5.2.1 3C 125

As shown in the XRT map in the 0.3–10 keV band (see Fig. 10, left panel) no X-ray emission has been detected for the source NVSS J044617+394503, within the positional uncertainty region of 3C 125. From the cross-match with the AllWISE Catalogue, we have found the source *WISE* J044617.88+394504.5 with an angular separation of 1.6 arcsec from the coordinates of the NVSS source. The infrared object is well detected in all four *WISE* filters; the *w1* image, given in the right panel of Fig. 10, shows good match between the positions of the radio and infrared sources, without evidence of confusion with other close objects. No information has been found in the literature regarding optical/infrared candidate counterparts for this radio source.

5.2.2 3C 139.2

The radio contours of a source classified as FR II (?) overlap the positional uncertainty region of 3C 139.2, and the NVSS object J050427+281255 is internal to it. From the cross-match of the NVSS with the AllWISE Catalogue we have obtained the infrared source *WISE* J052427.51+281256.7, well detected in all the four *WISE* filters, at an angular sep-

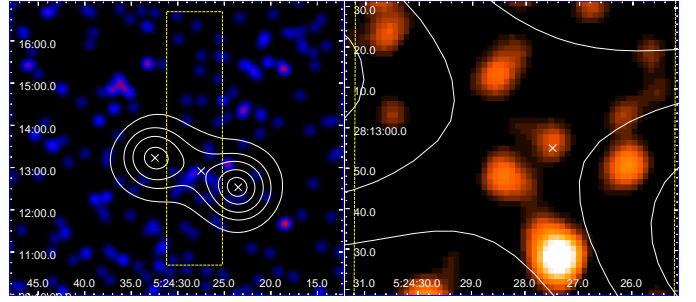


Figure 11. Same as Fig. 10 but for **3C 139.2**. White contours correspond in this case to 0.01, 0.08, 0.2, 0.4, and 0.6 Jy beam⁻¹.

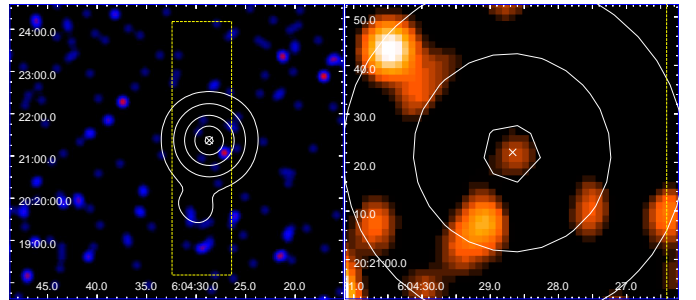


Figure 12. Same as Fig. 10 but for **3C 152**. White contours correspond in this case to 0.01, 0.1, 0.4, 0.9, and 1.3 Jy beam⁻¹.

aration of 1.5 arcsec. No information about infrared/optical identification has been found in the literature for 3C 139.2.

5.2.3 3C 152

The left panel of Fig. 12 shows the position of the source NVSS J060428+202122, at ~ 15 arcsec from the center of the positional uncertainty region of 3C 152, with no X-ray emission detected by XRT. From the cross-match with the AllWISE Catalogue we have found the source *WISE* J060428.62+202121.7, with an angular separation of only 0.8 arcsec between the two sources. The infrared object is well detected in three of the *WISE* filters, excluding *w4*. The image in the *w1* filter is given in the right panel of Fig. 12 and shows the good match between the positions of the radio and the infrared objects. In their analysis of the corresponding field of view with HST ? reported a single candidate (R.A.(J2000) 06^h 04^m 28^s.63, Dec.(J2000) +20° 21' 25".07). The angular separation of this object from *WISE* J060428.62+202121.7 is 3.4 arcsec.

5.2.4 3C 468.1

The left panel of Fig. 13 shows the position of the 1.4 GHz source NVSS J235054+644018 with respect to the positional uncertainty region of 3C 468.1. The *WISE* candidate J235054.78+644018.1, that we have found from the NVSS/AllWISE cross-match at an angular separation of 1.3 arcsec from the NVSS source, is detected in all the four *WISE* filters. ? presented the corresponding field of view as observed by HST and reported a list of three tentative optical identifications. Their source #1 (R.A.(J2000) 23^h 50^m

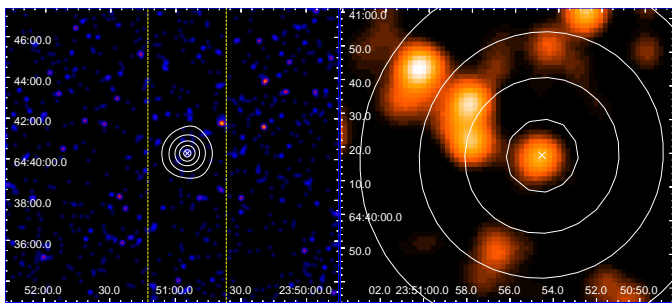


Figure 13. Same as Fig. 10 but for **3C 468.1**. White contours correspond in this case to 0.01, 0.2, 1.0, 2.2, and 3.3 Jy beam⁻¹.

$54^{\circ}.38$, Dec.(J2000) $+64^{\circ} 40' 18''.06$) is the closest (2.6 arcsec) to the *WISE* source addressed by our analysis. This value is consistent with the positional uncertainty (3 arcsec) they reported for all their candidates.

6 SUMMARY AND CONCLUSIONS

After conducting *Swift* observations of 21 bright NVSS sources corresponding to 3CR sources classified as unassociated in the third update of the 3CR catalogue, we have obtained new X-ray detections for nine of them. Moreover, cross-matching the NVSS with the recent AllWISE Catalogue, we have found a *WISE* counterpart to all these nine X-ray sources, as well as to four cases with no X-ray detection. We have provided candidate counterparts emitting in the infrared band for 3C 125, 3C 137, 3C 139.2, 3C 152, 3C 158, 3C 390, 3C 409, and 3C 454.2. Furthermore, we have confirmed an unambiguous association for 3C 86, 3C 91, 3C 131, 3C 428, and 3C 468.1 where multiple candidates had been suggested in previous analysis. Four of these infrared sources are listed in the recent all-sky catalogue of γ -ray blazar candidates (?): the infrared colours of these objects are similar to those of quasars (??), and only a spectroscopic campaign will reveal the real nature of these as well as of the remaining identified *WISE* counterparts.

It is worth mentioning that no optical/UV counterpart has been detected in the UVOT filters at the position of the 21 NVSS sources: this is in agreement with the notes reported in the 3CR catalogue (?) in which the large fraction of these 3CR unidentified radio sources were classified as *obscured* active galaxies. Therefore, our analysis suggests that a spectroscopic analysis in the infrared range will be more helpful to identify their nature as well as potentially obtain a redshift measurement.

ACKNOWLEDGEMENTS

The authors are grateful to the anonymous referee for helpful comments and suggestions. This work has been supported by ASI grant I/011/07/0. This research has made use of archival data, software or online services provided by the ASI Science Data Center; the High Energy Astrophysics Science Archive Research Center (HEASARC) provided by NASA's Goddard Space Flight Center; the SIMBAD database operated at CDS, Strasbourg, France; the NASA/IPAC Extragalactic

Database (NED) operated by the Jet Propulsion Laboratory, California Institute of Technology, under contract with the National Aeronautics and Space Administration. Part of this work is based on the NVSS (NRAO VLA Sky Survey): The National Radio Astronomy Observatory is operated by Associated Universities, Inc., under contract with the National Science Foundation and on the VLA low-frequency Sky Survey (VLSS). This publication makes use of data products from the Wide-field Infrared Survey Explorer, which is a joint project of the University of California, Los Angeles, and the Jet Propulsion Laboratory/California Institute of Technology, and NEOWISE, which is a project of the Jet Propulsion Laboratory/California Institute of Technology. WISE and NEOWISE are funded by the National Aeronautics and Space Administration. SAOImage DS9 were used extensively in this work for the preparation and manipulation of the images.

This paper has been typeset from a $\text{\TeX}/\text{\LaTeX}$ file prepared by the author.